# In-Situ Surface Inspection Using White Light Channelled Spectrum Interferometer

**X Jiang, D Tang and F Gao**

EPSRC Centre for Innovative Manufacturing in Advanced Metrology, University of Huddersfield, Huddersfield HD1 3DH, UK

E-mail: x.jiang@hud.ac.uk

**Abstract**. We introduce a new environmentally robust optical interferometry system for fast surface profile measurement. The proposed white light channelled spectrum Interferometer (WLCSI) is effective for applications in on-line surface inspection because it can obtain a surface profile in a single shot. Compared to the traditional spectral interferometry techniques, cylindrical lens is used in the Michelson interferometric objective of our system to achieve the measurement of long profiles. Combined with a modern high speed CCD camera, general-purpose graphics processing unit (GPGPU) and multi-core processors computing technology, large dynamic measurement with a high signal-to-noise ratio is realized. The designed prototype of WLCSI is presented and its performance was evaluated experimentally by measuring two surface samples. The measuring results closely align with the calibrated specifications given by the manufacturer as well as the measurement results by the other commercial instrument, which shows that the proposed WLCSI could be applied to production line like the roll-to-toll (R2R) surface inspection where only defects on the film surface are concerned in terms of the quality control.

## 1. Introduction

The rapidly developing industries such as Micro-Electro Mechanical System (MEMS) and micro optics, photovoltaic thin film and Si wafers require non-contact and high precision measurements [1]. Optical interferometry has been widely employed for its non-contact nature, which avoids the problem of generating applied loads and damaging the vulnerable tested surface. By using broadband illumination such as super-luminescent diodes and halogen lamps, white light interferometry (WLI) stands out from the wide range of optical-based techniques for overcoming the two pi phase ambiguity problem. It can be generally divided into three types, namely Vertical Scanning Interferometry (VSI) [2], Wavelength Scanning Interferometry (WSI) [3] and White Light Channelled Spectrum Interferometer (WLCSI), also called Spectrally Resolved White Light Interferometry (SRWLI) in other literatures [4].

Yet the VSI and the WSI are usually used in the off-line metrology field because they require the sample surface to remain stationary when performing measurements. For products like flexible photovoltaic (PV) modules and solar modules, large-area multi-layer thin films manufactured using R2R technology, defects may result from the coating and patterning processes. To achieve a high

product yield, precisely inspecting the foil surface at production speed is required. Therefore, it is desirable to employ an optical based on-line inspection system during PV manufacturing processes.

The WLCSI is a line profile measurement system eliminating the mechanical scanning. The mechanical movement is replaced by the spectral decomposition of the output of the spectrometer [5]. Obtaining a surface profile with a single interferogram makes it free from the requirements on the positioning and stability when the measurements are carried out on the shop floor and therefore has the potential to be used for in-situ surface inspection [6].

In this paper, we present an environmentally robust WLCSI system aimed at production line applications like R2R surface inspection where only defects on the film surface are concerned in terms of the quality control. Cylindrical lens is used as the interferometric objective to enable the measurement of long profiles. Michelson-type interferometer is selected so the aberrations resulting from the cylindrical lens can be well balanced. An initial prototype has been made and its performance was evaluated by measuring two surface samples. The captured white light interferograms were analyzed with a fast Fourier-transform (FFT) based algorithm and the results are discussed in detail.

## 2. Interferogram analysis in WLCSI

There are five steps to analyse the interferogram illuminated by white light, which are illustrated in detail in the following sections.

### *2.1. Removing background from the original signal*

Due to the influence from the spectral distribution of light source and the spectral response of CCD camera, it is known that the captured interferogram contains a background intensity variation. Therefore, we capture a reference frame without interference effect by blocking the measurement arm of the interferometer. The background intensity can then be obtained from this reference frame and removed from the corresponding spectral interferogram.

### *2.2. Wavelength calibration*

The white light interferogram is spectrally decomposed along the CCD pixels. The exact relationship between the pixel number and the specific wavelength needs to be calibrated. We used a white light laser source (WhiteLase™ micro) in conjunction with the acoustic-optical tunable filter (AOTF) for the calibration, in which much more spectral lines can be provided than a cadmium spectral lamp [6]. The specific wavelength selected by the AOTF is determined by

$$\lambda = \Delta n \alpha v_a * (f_a)^{-1} \tag{1}$$

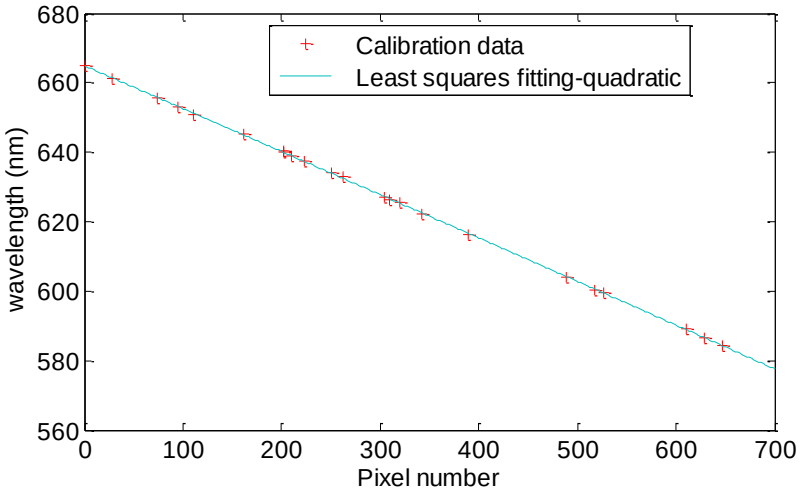


**Figure 1.** Wavelength calibration of the CCD camera

The relationship between pixel number and wavelength is represented as a second-order polynomial

$$\lambda_p = Ap^2 + Bp + C \tag{2}$$

where $\lambda_p$ is the wavelength of pixel $p$, $C$ is the wavelength of pixel 0, $B$ is the first coefficient (*nm/pixel*) and $A$ is the second coefficient (nm/ pixel$^2$). 20 spectral lines were used to calculate the value for *A, B* and *C* through least squares equation. The calibration result is depicted in Figure 1.

*2.3. Coordinate transformation*

A two-dimensional CCD detector is used to record the interference signal, with one axis (horizontal) being used to provide the phase information encoded as a function of wavenumber, and the other (vertical) being used to give the length of the measured surface profile [7]. Nevertheless, the original channelled spectrum is registered by the CCD with respect to the pixel number (or wavelength $\lambda$). While the phase variation in the spectral interferogram is linearly related to the wavenumber ($\sigma = 1/\lambda$), so coordinate transformation is required. More specifically, firstly the data matrix **M**($p$, $\lambda$) is converted to a new data matrix **N**($p$, $\sigma$), then the matrix **N** is resampled in equal intervals through interpolation and finally the original sinusoidal signals is reconstructed to a wavenumber related curve. Hence, the spectral intensity I $(\mathrm{h}, \sigma)$ recorded at the output of the spectrometer can be expressed as

$$\bar{I}(x, y; \sigma) = a(x, y; \sigma) + b\,(x, y; \sigma)\cos[\varphi(x, y; \sigma)] \tag{3}$$

where $\bar{I}(x, y; \sigma)$ is the normalized intensity with background intensity variation removed, $(x, y)$ denotes the spatial coordinates of interferogram, $a(x, y; \sigma)$ and $b(x, y; \sigma)$ represent the background intensity and fringe visibility, respectively; and the phase $\varphi(x, y; \sigma)$ is defined by formula

$$\varphi(x, y; \sigma) = \frac{4\pi}{\lambda} \times h(x, y) + \varphi_0 = 4\pi\sigma h(x, y) + \varphi_0 \tag{4}$$

where $h(x, y)$ represents the surface elevation, $\varphi_0$ is the initial phase.

*2.4. Phase calculation*

There are many algorithms to extract the phase from the spectral interferogram, covering the techniques based on FFT [8], convolution [9] and Hilbert transform [10], etc. We developed a FFT based algorithm because it is effective, accurate and insensitive to intensity noise [11].

$$\bar{I}(x, y; \sigma) = a(x, y; \sigma) + c(x, y; \sigma) + c^*(x, y; \sigma) \tag{5}$$

with

$$c(x, y; \sigma) = \frac{1}{2} b\,(x, y; \sigma)\exp[i\,\varphi(x, y; \sigma)] \tag{6}$$

where $*$ denotes a complex conjugate. After Fourier transform, the original spatial signals are analysed in frequency domain and equation (3) can be written as

$$\tilde{I}(x, y; f) = A(x, y; f) + C(x, y; f) + C^*(x, y; f) \tag{7}$$

where the capital letters denote the Fourier spectra and $f$ is the spatial frequency. The unwanted background variation is removed by setting a filtration window, and then the desired term $\mathrm{C}(x, y; f)$ is

selected to compute the inverse fast Fourier transform (IFFT). Taking the natural logarithm of the IFFT$[C(x,y;f)]$, finally the phase $\varphi(x,y;\sigma)$ of each point is extracted as the imaginary part of the equation (8)

$$\log\{\tfrac{1}{2}b\,(x,y;\sigma)\,\exp[i\,\varphi(x,y;\sigma)]\} = \log\,[\tfrac{1}{2}b(x,y;\sigma)] + i\,\varphi(x,y;\sigma) \tag{8}$$

Figure 2(a) shows the wrapped phase. The corrected continuous phase can be obtained by using the method illustrated by Takeda et. al [8]. From the equation (4), the phase variation is linearly related to the wavenumber, therefore the unwrapped phase slope is fitted using least squares method, as shown in Figure 2(b).

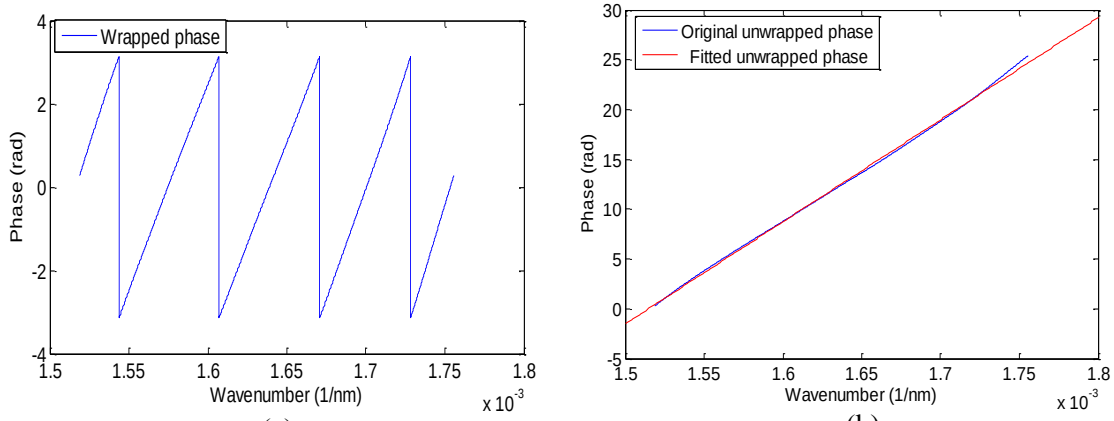


(a) (b)

**Figure 2.** Phase profile of the white light interferogram: (a) Wrapped phase. (b) Unwrapped phase

*2.5. Height map of a one-dimensional profile*

As mentioned above, the vertical axis of the interference signal represents one dimension of lateral resolution, which means each row signal contains the height information of one point. The height value is calculated from the phase slope *S*, which is expressed as equation (9). After analysis of a series of row signals, then the height map of a surface profile can be acquired.

$$h = \frac{S}{4\pi} = \Delta\varphi * [4\pi(\sigma_m - \sigma_n)]^{-1} \tag{9}$$

## 3. Experimental setup and initial prototype

*3.1. Experimental setup of proposed system*

The basic configuration of the in-situ surface inspection system is illustrated in Figure 3. A halogen bulb with broadband spectrum provides the white light illumination for the system, which is coupled into a multi-mode optical fibre patch cable with a numerical aperture of 0.39. The tested surface is observed through a cylindrical lens based Michelson interferometric objective. The measurement of long profiles can be achieved due to the imaging property of the cylindrical lens. The interference beam passes through a slit to block the light that is redundant for measurement. That is to say, for each measurement only a narrow line of light which represents an interference signal of a surface profile is selected, then diffracted by the grating and finally received on a CCD camera. After wavelength calibration wavenumber σ spreads along the chromaticity axis in a range of 1.50 $\mu m^{-1}$ 1.71 $\mu m^{-1}$. The direction of the slit is set to be parallel to the columns of CCD pixels, so that the dispersion axis is along the rows. The CCD camera (ICL-B0620 from Imperx) has a resolution of 648 x 488 pixels and a frame rate of 208 fps in normal working condition. The prototype of WLCSI is shown in Figure 4,

which has a size of 468mm x 140mm x 91mm (length x width x height). Four mounting holes were made on the prototype base so that it is convenient to be embedded into an industrial machine.

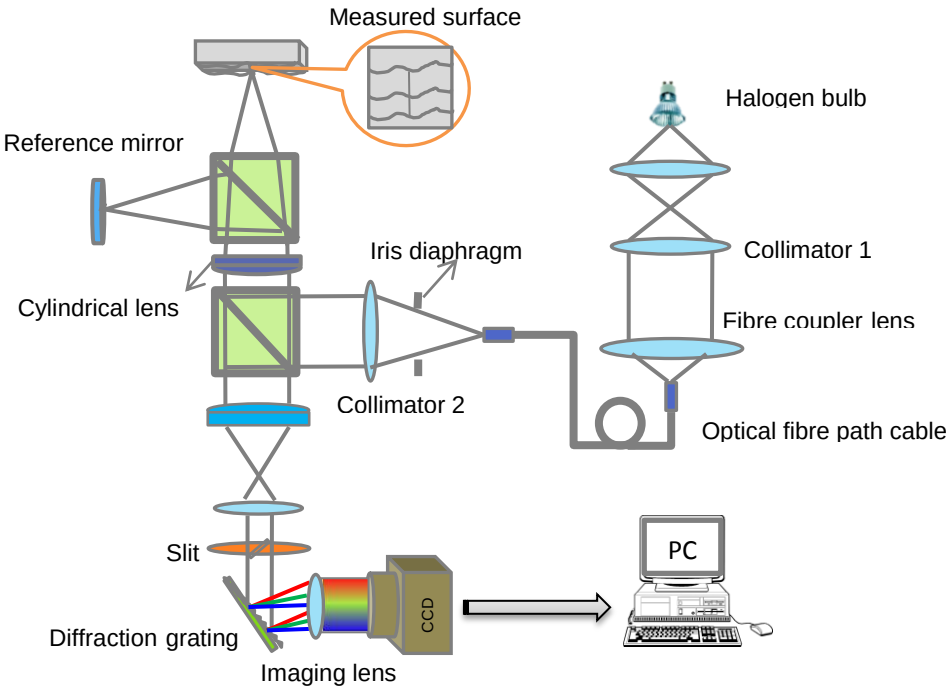


**Figure 3.** Schematic diagram of WLCSI

*3.2. Measurable heights range of WLCSI*

When the measurement is performed, the sample should be placed within the depth of field (DOF) of the objective to resolve the details of the tested surface. Fringes still can be observed as the optical path difference (OPD) between the tested surface and reference surface exceeds the DOF, the visibility of the fringes and the signal-to-noise of the interference output, however, greatly decreased and eventually no interference exist when the OPD is greater than the coherence length. Therefore, the measurement range is related directly to the DOF and coherence length, and determined by the smaller of these two numbers. The depth of field is defined by:

$$DOF = \lambda(1 - NA^2)^{1/2} NA^{-2} \tag{10}$$

The coherence length is expressed as

$$l_c = \frac{k\lambda^2}{\Delta\lambda} \tag{11}$$

where $k$ is the correction factor depending on spectral profile. For the Gaussian distribution and Lorentzian distribution, $k$ is equal to 0.32 and 0.66, respectively. As for the WLCSI, the coherence length is much greater than the DOF due to the function of the spectrometer. Therefore, the measurable heights range is limited by the DOF, which is theoretically approximately 144 µm.

## 4. Results and discussion

Two surface samples were measured to evaluate the performance of the WLCSI prototype. Figure 5 is a 30 µm standard sample manufactured by Rubert & Co. Ltd.. By translating the sample in the direction that is perpendicular to the tested profile, in-situ surface inspection was simulated. Figure 5(a) and Figure 5(b) shows the obtained three-dimensional surface map (constructed by 800 profiles) and

the cross-sectional plot of the step, respectively. To make a comparison, the commercial instrument Talysurf CCI 3000 was used to measure almost the same area of the sample as shown in Figure 6.

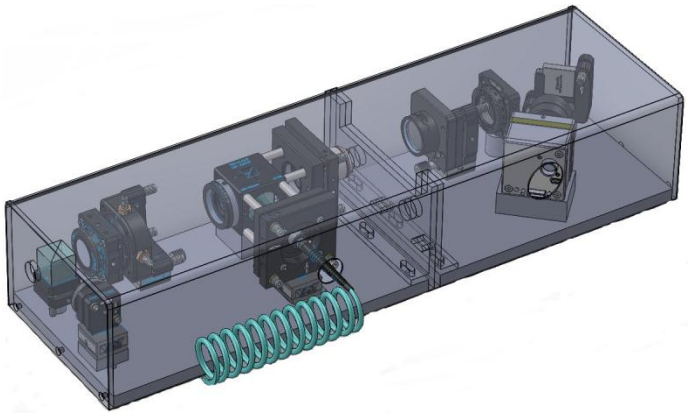

**Figure 4.** Initial prototype of WLCSI

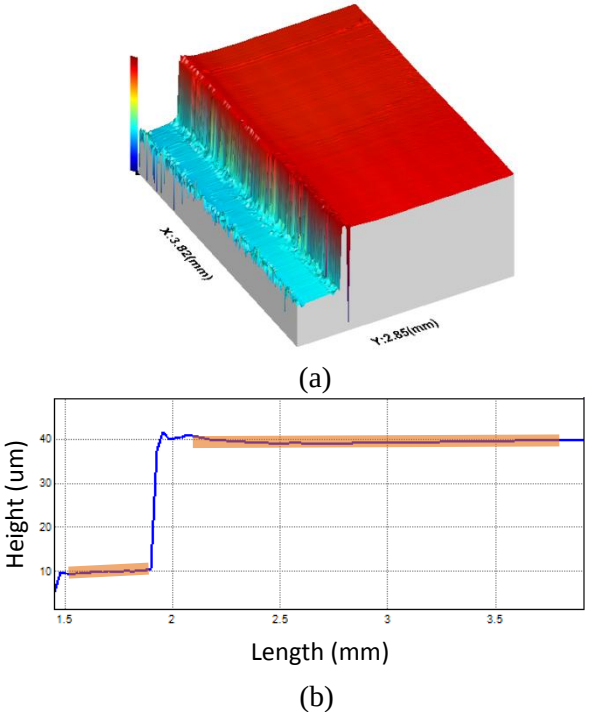


**Figure 5.** Measurement result of a 30 µm step height sample (WLCSI): (a) 3D surface map, (b) cross-sectional profile.

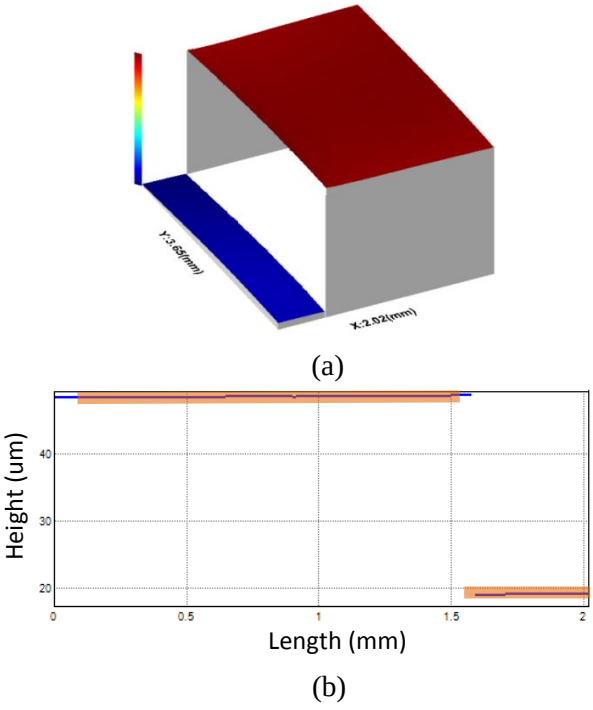


**Figure 6.** Measurement result of a 30 µm step height sample (CCI): (a) 3D surface map, (b) cross-sectional profile.

The 3D surface map obtained from the WLCSI is constructed by many profiles with different positions of the tested area. Therefore it will not be as flat as that of from CCI. We compared the average step heights of this area, which have been calculated as 29.431 µm and 29.278 µm corresponding to CCI and the WLSCI, respectively. Those two close results demonstrate that our WLCSI prototype has the sufficient resolution for the precision surface profile measurement.

The other sample is a defective mirror with a scratch. The flatness of this mirror given by the manufacturer is less than $\lambda/10$ (@ 633 nm), which is confirmed by measuring the non-damaged area

with our setup. Figure 7 shows a profile of the surface measured at the area without any damage. When the sample was scanned through, the scratch was detected and the interferogram is shown in Figure 8. Figure 9 shows the results of this scratch. As we can see, many speckle errors occur at the scratch edge, which may produce false information during the measurement. The most likely reason is that the defect edge formed an accumulation due to the squeeze. The other possible reason is the batwing effect which is a problem usually for the surface heights are smaller than the coherence length of the white light [12]. The measurement results using CCI provided the similar results which testify the reliability of the measurement using WLCSI, as shown in Figure 10. The acquired measurement results of the defective mirror further demonstrate the WLSCI prototype is capable of being applied to production line like the R2R surface inspection where only defects on the film surface are concerned in terms of the quality control.

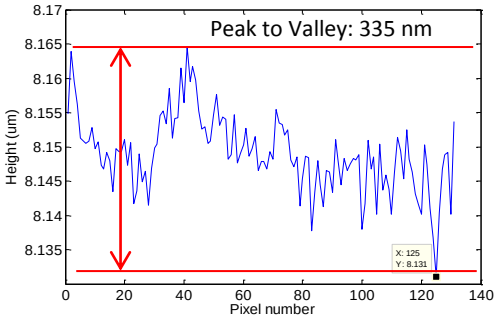


**Figure 7.** One profile of the mirror surface

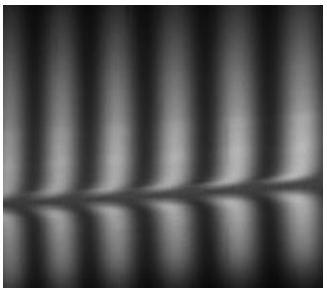

**Figure 8.** Interferogram of the defect

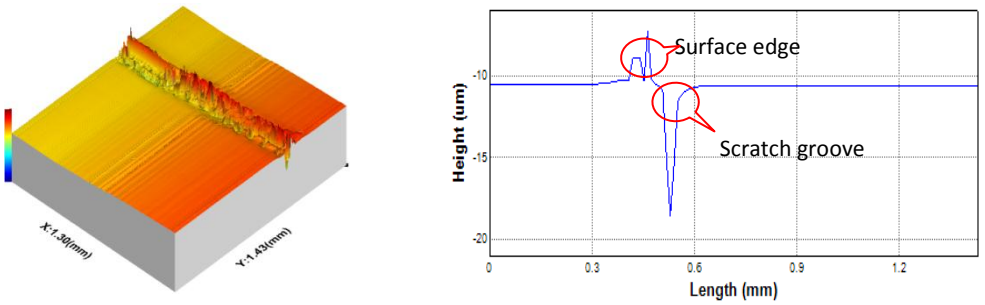


(a) (b)

**Figure 9.** Measurement results of a scratch (WLCSI): (a) 3D surface map, (b) cross-sectional profile.

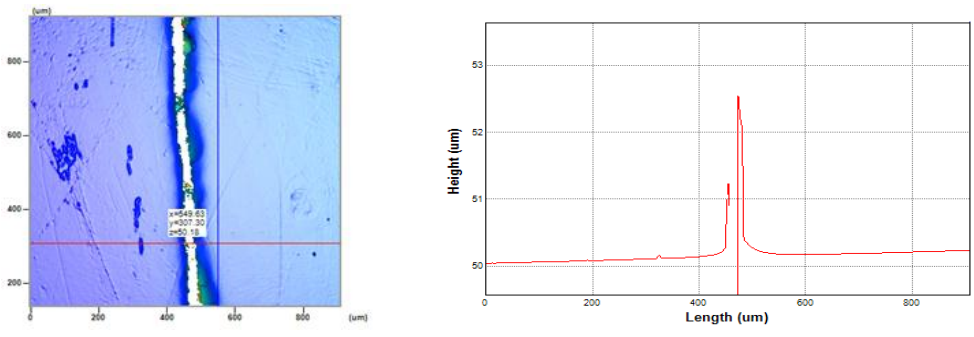


(a) (b)

**Figure 10.** Measurement results of a scratch (CCI): (a) 3D surface map, (b) cross-sectional profile.

## 5. Conclusions

A white light channelled spectrum Interferometer aimed at in-situ surface inspection is presented. Obtaining a surface profile in a single shot allows this setup to minimise the effect of external perturbations and environmental noise when it is employed on the shop floor. The initial prototype was made and its performance was evaluated experimentally by measuring two samples. The measurement results acquired using both the WLCSI prototype and commercial instrument CCI align with each other acceptably. By integration of a modern high speed CCD camera, general-purpose graphics processing unit (GPGPU) and multi-core processors computing technology, the required time for frame grabbing and data processing can be greatly shortened which will enable this cylindrical based WLCSI system to be qualified for the real-time surface measurement.

The authors gratefully acknowledge the UK's Engineering and Physical Sciences Research Council (EPSRC) funding of the First Grant (Grant Ref: EP/K007068/1), the funding of EPSRC Centre for Innovative Manufacturing in Advanced Metrology (Grant Ref: EP/I033424/1) and the funding with Grant Ref: EP/K018345/1.

## References

[1] Maboudian R 1998 Surface processes in MEMS technology *Surf. Sci. Rep.* **30** 207-269

[2] Scott C C, Luttge A and Athanasiou K A 2005 Development and validation of vertical scanning interferometry as a novel method for acquiring chondrocyte geometry *J Biomed Mater Res* A **72** 83-90

[3] Gao F, Muhamedsalih H and Jiang X 2012 Surface and thickness measurement of a transparent film using wavelength scanning interferometry *Opt. Express* **20** 21450-21456

[4] Y Ghim and S Kim 2009 Spectrally resolved white-light interferometry for 3D inspection of a thin-film layer structure *Appl. Opt.* **48** 799-803

[5] Mehta D S, Saito S, Hinosugi H, Takeda M and Kurokawa T 2003 Spectral interference Mirau microscope with an acousto-optic tunable filter for three-dimensional surface profilometry. *Appl. Opt.* **42**1296-1305

[6] D Tang, F Gao and X Jiang 2014 On-line surface inspection using cylindrical lens-based spectral domain low-coherence interferometry *Appl. Opt.* **53** 5510-5516

[7] Hart M, Vass D G and Begbie M L 1998 Fast surface profiling by spectral analysis of white-light interferograms with Fourier transform spectroscopy *Appl. Opt.* **37**1764-1769

[8] Takeda M, H Ina and S Kobayashi 1982 Fourier-transform method of fringe-pattern analysis for computer-based topography and interferometry *J. Opt. Soc. Am.* **72** 156-160

[9] Sainz C, J Calatroni and G Tribillon 1990 Refractometry of liquid samples with spectrally resolved white light interferometry *Meas. Sci. Technol.* **1** 356-361

[10] Debnath S K and M P Kothiyal 2006 Analysis of spectrally resolved white light interferometry by Hilbert transform method *Proc. SPIE* **6292** 62920P

[11] Jiang X, Wang K, Gao F and Muhamedsalih H 2010 Fast surface measurement using wavelength scanning interferometry with compensation of environmental noise *Appl. Opt.* **49** 2903-2909

[12] Debnath S K and M P Kothiyal 2006 Improved optical profiling using the spectral phase in spectrally resolved white-light interferometry *Appl. Opt.* **45** 6965-6972